Published in Applied Physics Letters 83, 1929-1931, 2003
which should be used for any reference to this work

Continuous-wave distributed-feedback quantum-cascade lasers on a Peltier cooler

Thierry Aellen,[a] Stéphane Blaser,[b] Mattias Beck, Daniel Hofstetter, and Jérôme Faist[c]
Institute of Physics, University of Neuchâtel, CH-2000 Neuchâtel, Switzerland

Emilio Gini
FIRST Center for Micro- and Nanoscience, Swiss Federal Institute of Technology, CH-8093 Zurich, Switzerland

Continuous-wave operation of $\lambda \sim 9\ \mu$m distributed-feedback quantum-cascade lasers is reported up to a temperature of 260 K. Single-frequency emission with a side mode suppression ratio of $\geqslant 27$ dB and with a tuning range of 5 cm^{-1} between 200 and 245 K (a tunability of $-0.078\ \mathrm{cm}^{-1}/\mathrm{K}$ and $-0.764\ \mathrm{cm}^{-1}/\mathrm{W}$) is obtained for the junction-down mounted buried heterostructure devices. Uncoated lasers display an output power of up to 18 mW at 180 K and still 1 mW at 250 K. Lasers with high-reflection coated facets could be operated up to 260 K.

The ability to match the emission frequency of quantum-cascade (QC) lasers to the fundamental absorption bands of molecular trace gas species in the midinfrared offers an attractive option for gas sensing applications. In addition, this type of semiconductor laser recently demonstrated continuous-wave (cw) operation at room temperature with output powers of some milliwatts[1] indicating its potential for compact, sensitive and highly selective sensor systems. QC lasers with an incorporated distributed feedback (DFB) grating are of particular interest to most high-resolution spectroscopy applications requiring tunable single-frequency light sources with a narrow linewidth. Up to now, cw operation of DFB QC lasers was reported in the wavelength range from $\lambda = 4.6\text{–}11.8\ \mu\mathrm{m}$[2–6] for temperatures $\leqslant 120$ K. Gas sensing applications such as absorption spectroscopy of NO and NH_3[7] or trace gas analysis[8,9] would potentially benefit from compact DFB QC sources operating in cw mode at noncryogenic temperatures.

In this letter, we report the realization of first order DFB QC lasers with cw operation on a thermoelectric cooler at an emission frequency of $\nu \sim 1115\ \mathrm{cm}^{-1}$. The lasers are based on a double-phonon resonance active region[10] and fabricated as narrow stripe, planarized, buried heterostructure devices[11] in which the active region is vertically and laterally surrounded by InP allowing heat extraction towards all sides of the active region. Our laser structure is identical to the one described in Ref. 1; fabrication and mounting of the lasers followed the same procedure as described therein with the difference of the additional DFB grating. Figure 1(a) shows schematically a junction-down mounted QC laser with the DFB grating etched into the upper InGaAs layer on top of the active laser core before regrowth of the InP top cladding. The DFB grating with a period of $\Lambda = 1.43\ \mu$m was holographically defined and etched in the InGaAs waveguide layer with the solution $H_3PO_4:H_2O_2:H_2O$ (2:4:6) to a depth of 180 nm. The top width of the laser stripe is somewhat narrower than previously published but the laser ridge exhibits a strong trapezoidal shape (6–8 μm on top and more than 18 μm on the bottom of the active region, as measured with an optical microscope). This trapezoidal shape is due to the heavely aged wet etchant resulting in inhomogeneous etch rates (laterally and vertically) of the different constituant ma-

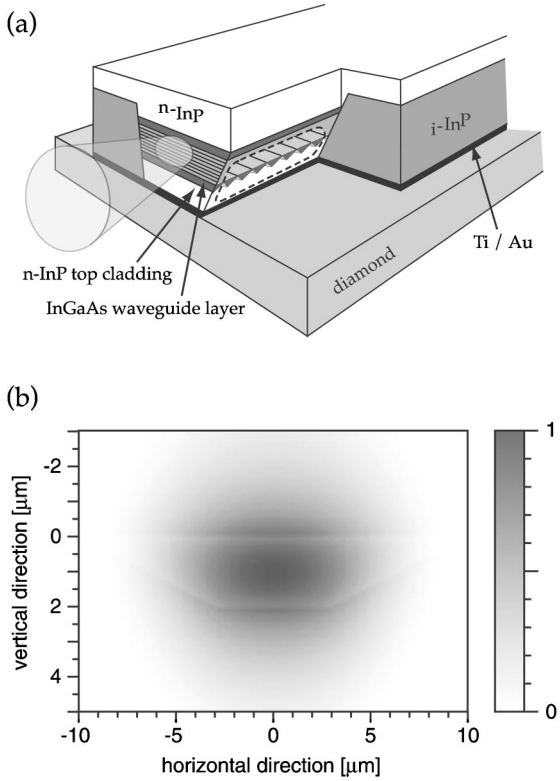

FIG. 1. (a) Schematic view of the junction-down mounted QC–DFB device soldered on a diamond platelet. The lateral *i*-InP layer was partially removed to show the DFB grating etched in the InGaAs waveguide layer. (b) Computed transverse fundamental mode profile in a mode amplitude scale using a trapezoidal shape for the active region.

[a]Electronic address: thierry.aellen@unine.ch
[b]Present address: Alpes Lasers SA, 1-3 Maximilien-de-Meuron, CH-2000 Neuchâtel, Switzerland.
[c]Electronic address: jerome.faist@unine.ch

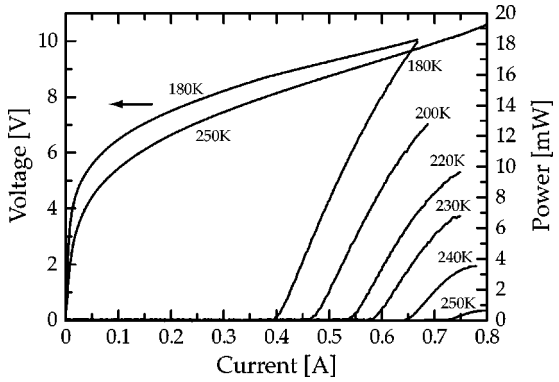

FIG. 2. Voltage and optical power vs current of a 1.5 mm long uncoated DFB laser operated in cw mode at various heat sink temperatures between 180 and 250 K.

terials. Figure 1(b) shows the computed transverse mode profile using a commercial beam-propagation software.[12] Using the trapezoidal shape of the active region, the refractive index and the overlap factor resulting from the calculation are respectively $n_{\text{eff}}=3.18$ and $\Gamma=46\%$.

To enable a large temperature tuning range, lasers were mounted on the cold finger of a N_2-flow cryostat. The light from the facet was collected by a $f/0.8$ optics and the output power was measured with a calibrated thermopile detector. Figure 2 shows voltage bias and cw optical output power collected from one facet of a 1.5 mm long junction-down mounted DFB laser. The laser emitted 18 mW of optical power and exhibited a threshold current of 400 mA and a slope efficiency dP/dI of 78 mW/A at $T=180$ K. The threshold current increased up to 730 mA for the maximum operating temperature of $T=250$ K for continuous wave operation, while the optical power was still 0.6 mW at 790 mA.

The emission of the laser can usually be tuned by changing either current or temperature. A series of cw spectra was collected using a high-resolution ($0.125\ \text{cm}^{-1}$) Fourier-transform infrared spectrometer and a deuterated triglycine sulphate detector. Single-mode emission was observed with a sidemode suppression ratio (SMSR) of $\geqslant 27$ dB for the entire investigated temperature and current range as shown in Fig. 3. The full width at half maximum is narrower than $0.125\ \text{cm}^{-1}$, limited by the spectrometer resolution. The emission spectra measured at a constant injection current of 680 mA and at different temperatures between 180 and 245 K revealed a linear tuning of the center frequency from 1116.80 to $1113.63\ \text{cm}^{-1}$ with the tuning coefficient $(1/\nu)(\Delta\nu/\Delta T)=-6.98\times10^{-5}\ \text{K}^{-1}$. The refractive index deduced using the Bragg wavelength λ_B and extrapolated to room temperature using this tuning coefficient is $n_{\text{eff}}=\lambda_B/2\Lambda=3.14$. The difference with the theoretical value of $n_{\text{eff}}=3.18$ calculated with the software is attributed to an uncertainty in the refractive index of each individual layer and the evaluation of the Bragg wavelength. At a constant temperature of 203 K, the emission frequency shifts from 1118.48 to $1116.80\ \text{cm}^{-1}$ for various drive currents ranging from 500 to 680 mA with a linear tuning coefficient of $\Delta\nu/\Delta P=-0.764\ \text{cm}^{-1}\,\text{W}^{-1}$. Since the emission frequency is a function of the temperature (which changes the averaged refractive index across the entire laser structure), we can deduce a thermal resistance R_{th} of the device with

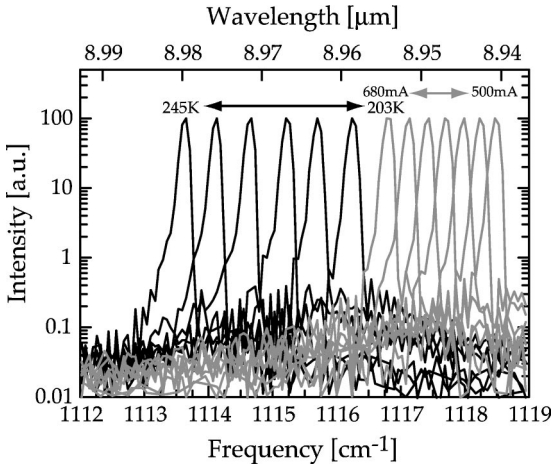

FIG. 3. Series of high resolution cw spectra of the 1.5 mm long uncoated DFB device as a function of the temperature ($T=203$, 212, 219, 225, 232, 239, and 245 K) at a constant drive current of 680 mA (black curves) and as a function of various drive currents ranging between 500 and 680 mA in steps of 30 mA at a constant temperature of 203 K (gray curves). The curves are normalized to the emission spectrum measured at 203 K, 680 mA. We deduced the two linear tuning coefficients $\Delta\nu/\Delta T=-0.078\ \text{cm}^{-1}/\text{K}$ and $\Delta\nu/\Delta P=-0.764\ \text{cm}^{-1}\,\text{W}^{-1}$.

the above tuning coefficients using $R_{\text{th}}=\Delta T/\Delta P=\Delta\nu/\Delta P\cdot(\Delta\nu/\Delta T)^{-1}$ and find $R_{\text{th}}=9.8$ K/W.

In pulsed mode at low duty cycle, heating effects are negligible. In cw operation, however, the active region temperature T_{act} is much higher than the heat sink temperature T_{sink} due to the high heat dissipation during lasing action; T_{act} can be related to the heat sink temperature by the thermal resistance R_{th}, the voltage U and the threshold current I_{th} with $T_{\text{act}}=T_{\text{sink}}+U\cdot I_{\text{th}}\cdot R_{\text{th}}$. Following the model derived in our previous article,[1] the temperature dependence of the cw threshold current can then be predicted from the one measured in pulsed mode. The result of this procedure is displayed in Fig. 4. The small discrepancy between the calculated cw threshold current and the calculated curve is probably due to the strong trapezoidal shape of the laser. The effective index of the optical modes depends on a weighted average of the temperatures of the whole structure (including claddings), whereas the threshold current density will be

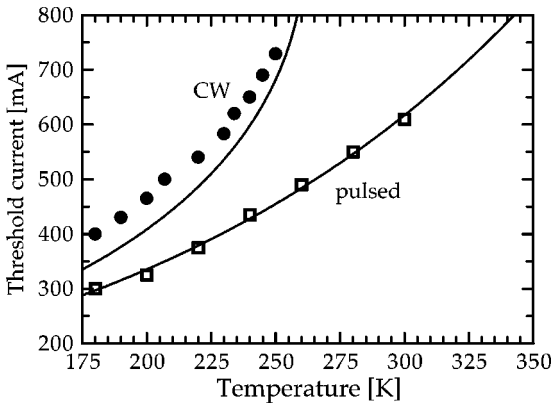

FIG. 4. Threshold current as a function of heat sink temperature. The experimental pulsed data (open squares) are fitted by the relation $I_{\text{th}}=I_0\cdot\exp(T_{\text{act}}/T_0)$, with a characteristic temperature $T_0=164$ K and $I_0=99$ mA (lower solid line). Solid circles represent experimental cw threshold currents. The upper solid line is the dependence of the cw threshold current as a function of the heat sink temperature computed from the thermal model.

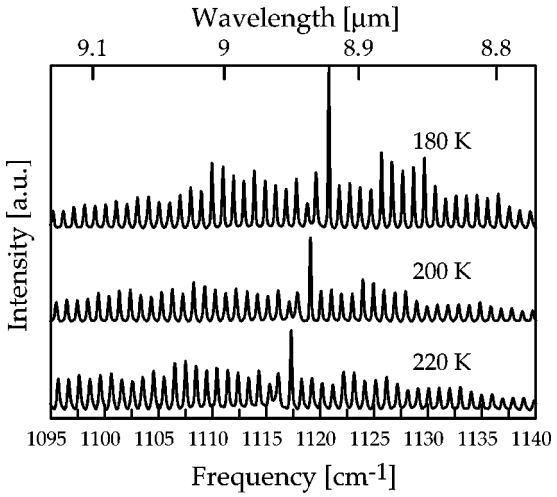

FIG. 5. Subthreshold cw luminescence spectra at 180, 200, and 220 K. The curves are vertically displaced for clarity.

controlled by the active region temperature only. For such a shape, this makes the effective thermal resistance of the device higher than the one extracted from the spectra. Moreover, narrow stripes will potentially lead to an increase of the top contact resistance and to leakage currents. These effects can also explain the slightly worse temperature behavior and the higher voltage bias of the DFB lasers compared to the Fabry–Pérot (FP) lasers fabricated with the same epilayer.[1]

In Fig. 5 are displayed subthreshold continuous-wave luminescence spectra of the same device at 180, 200, and 220 K. The envelop of the Fabry–Pérot franges is centered at about 1116 cm^{-1} with a spacing of the Fabry–Pérot modes of 0.98 cm^{-1}. The Bragg reflector's stopband width is $\Delta(1/\lambda)=1.19$ cm^{-1} and located at 1120.3 (180 K), 1119.0 (200 K), and 1117.2 cm^{-1} (220 K). This allows us to deduce a grating coupling coefficient of $\kappa=\Delta\lambda\pi n_{\mathrm{eff}}/\lambda^2=12$ cm^{-1}, using the experimental value of $n_{\mathrm{eff}}=3.14$. Based on the modal refractive index difference $\Delta n_{\mathrm{eff}}=1.1\times10^{-2}$ (calculated using the beam-propagation software),[12] we obtain $\kappa=\Delta n_{\mathrm{eff}}\pi/2\lambda=19$ cm^{-1}. The higher calculated value can be attributed to nonideal trapezoidal grating shape with less than 50% duty cycle. With the length of the device ($L=1.5$ mm), we get $\kappa L=1.8$ corresponding to a good single-mode operation efficiency and a SMSR of 30 dB [13] as obtained experimentally.

Because of the trapezoidal cross-section of the laser ridge, normalization of the usual laser parameters such as threshold current density per unit area is somewhat arbitrary. As a comparison, the FP lasers from the same epilayer,[1] using the same mounting and fabrication procedure, exhibit a linear dependent threshold current with laser width between 12 and 28 μm. The threshold current of the DFB laser reported here is comparable to a laser of 9–10 μm width accepting such a linear behavior. But assuming the electrical scaling of the current density versus the voltage curves with the FP lasers, the width of the DFB laser is estimated to 6–7 μm, which actually corresponds to the top active region width. The higher threshold current can be explained by the reduced overlap factor Γ (46%) of the strong trapezoidal shape (see earlier) compared with the FP lasers ($\Gamma=56\%$). Finally, supposing an identical thermal conductance as found for the FP lasers [$G_{\mathrm{th}}=574$ W/(K cm^2)], the thermal resistance of the DFB laser ($R_{\mathrm{th}}=9.8$ K/W) gives a laser width of 11–12 μm. This higher value can be attributed to a large contact area between the active region and the lateral InP regrowth resulting in a higher heat dissipation.

To reduce threshold current and to increase operating temperatures, another 1.5 mm long DFB device was facet coated after soldering with a high-reflection pair of Al_2O_3/Ge layers (about 1.3 and 0.6 μm, respectively), resulting in a facet reflectivity of $R\sim0.86$. Under pulsed operation, threshold current at room temperature decreased from 690 mA for the uncoated device to 620 mA after back-facet coating and down to 530 mA for the same device with both facets coated. Under cw operation at 200 K, the back-facet coated device showed lasing action above a threshold of 465 mA and emitted 30 mW of optical power at $I=740$ mA. The corresponding values of the double-side coated device are $I_{\mathrm{th}}=395$ mA and $P_{\mathrm{opt}}=6$ mW at $I=720$ mA under these operating conditions. The maximum cw operating temperature of the single-side coated device was 245 K with $P_{\mathrm{opt}}=3$ mW, whereas the device with back and front facet coating could be operated up to 260 K with some tens of μW at $I=870$ mA.

In conclusion, we have demonstrated continuous wave single-mode operation of buried heterostructure DFB QC lasers at temperatures easily reachable with a Peltier cooler.

The authors would like to thank Daniel Gerber for his help in software simulations. This work was financially supported by the Swiss National Science Foundation and the Science Foundation of the European Community under IST project SUPERSMILE.

[1] M. Beck, D. Hofstetter, T. Aellen, J. Faist, U. Oesterle, M. Ilegems, E. Gini, and H. Melchior, Science (Washington, DC, U.S.) **295**, 301 (2002).
[2] R. Köhler, C. Gmachl, A. Tredicucci, F. Capasso, D. Sivco, S. Chu, and A. Cho, Appl. Phys. Lett. **76**, 1092 (2000).
[3] C. Gmachl, F. Capasso, A. Tredicucci, D. Sivco, J. Baillargeon, A. Hutchinson, and A. Cho, Opt. Lett. **25**, 230 (2000).
[4] C. Gmachl, A. Straub, R. Colombelli, F. Capasso, D. Sivco, A. Sergent, and A. Cho, IEEE J. Quantum Electron. **38**, 569 (2002).
[5] C. Gmachl, F. Capasso, J. Faist, A. Hutchinson, A. Tredicucci, D. Sivco, J. Baillargeon, S. Chu, and A. Cho, Appl. Phys. Lett. **72**, 1430 (1998).
[6] W. Schrenk, N. Finger, S. Gianordoli, E. Gornik, and G. Strasser, Appl. Phys. Lett. **77**, 3328 (2000).
[7] S. Sharpe, J. Kelly, J. Hartmann, C. Gmachl, F. Capasso, D. Sivco, J. Baillargeon, and A. Cho, Opt. Lett. **23**, 1396 (1998).
[8] A. Kosterev, R. Curl, F. Tittel, C. Gmachl, F. Capasso, D. Sivco, J. Baillargeon, A. Hutchinson, and A. Cho, Opt. Lett. **24**, 1762 (1999).
[9] A. Kosterev and F. Tittel, IEEE J. Quantum Electron. **38**, 582 (2002).
[10] D. Hofstetter, M. Beck, T. Aellen, and J. Faist, Appl. Phys. Lett. **78**, 396 (2001).
[11] M. Beck, J. Faist, U. Oesterle, M. Ilegems, E. Gini, and H. Melchior, IEEE Photonics Technol. Lett. **12**, 1450 (2000).
[12] BeamPROP™ version 5.0, RSoft Design Group, Inc.
[13] H. Kogelnik and C. Shank, J. Appl. Phys. **43**, 2327 (1972).